Photoinduced Birefringence and Surface Relief Gratings in Polyurethane Elastomers with Azobenzene Chromophore in the Hard Segment

Yiliang Wu,[†,‡] Almeria Natansohn,[†,§] and Paul Rochon*[,||]

Department of Chemistry, Queen's University, Kingston, Ontario, Canada K7L 3N6, and Department of Physics, Royal Military College, Kingston, Ontario, Canada K7K 5L0

Received March 26, 2004; Revised Manuscript Received May 20, 2004

ABSTRACT: A series of polyurethane elastomers containing aromatic azobenzene chromophore in the hard segment was synthesized by a one-step method. AFM surface study showed that particles on the order of 100 nm to several micrometers appeared after annealing the polymer films. Birefringence was induced in these polymer elastomers. The stability of the photoinduced birefringence could be improved significantly by annealing the polymer films. This also induced microphase separation. The effects of azo contents and molecular weight of soft segments were investigated. Dynamic study shows that photoinducing rate decreased while relaxation rate increased after annealing. Surface relief gratings could be induced only on the pure polyurethane and the elastomer containing 75% bis(azo)−diol. Only a reversible volume hologram was observed for the other elastomers.

Introduction

In recent years azobenzene-containing organic and polymeric materials have been the subject of intensive research due to their potential applications in photonics. Birefringence and surface relief gratings can be optically induced in various forms of these materials, such as polymer matrixes doped with azo dyes,[1,2] liquid-crystalline azopolymers,[3−7] and amorphous azopolymers.[8−10] Irradiation with linearly polarized light induces a macroscopic alignment of the azobenzene groups with their molecular long axis perpendicular to the polarization direction of the incident light. This is thought to be a result of multiple trans−cis−trans photoisomerization cycles. In addition irradiation with coherent interfering laser beams generates sinusoidal surface relief gratings as a result of massive movement of the polymer material.

Previous studies in our laboratory have demonstrated that large birefringence and deep surface relief gratings could be induced in amorphous polymers with relatively high glass transition temperatures (T_g).[11] The amorphous homopolymers and copolymers studied so far were homogeneous systems.[11] Heterogeneous systems with azobenzene groups located in a phase separated from the matrix may allow better three-dimensional optical access. Given a photoactive phase that is well dispersed within an "inert" matrix, we can prepare samples with low absorbance but with high local concentration of azobenzene groups for three-dimensional optical storage. Moreover, the study of the phase-separated systems might help us understand the mechanism for surface relief grating formation.

Segmented polyurethane with alternating sequences of hard and soft segments is an important class of thermoplastic elastomers.[12,13] The thermodynamic incompatibility between the hard and soft segments normally results in a microphase-separated structure. Therefore, a simple way to develop the phase-separated materials is to incorporate azobenzene groups into the hard segment of a polyurethane elastomer. The distribution of the hard segments can be tailored by controlling the ratio of the hard to soft segments and the length of the soft segment. Furthermore, the soft segment can be easily designed to be optically transparent. In this study, a series of polyurethane elastomers was synthesized and characterized. Photoinduced birefringence was investigated as a function of length and feed ratio of the soft segment. Holographic gratings were examined on these heterogeneous systems.

Experimental Section

The synthesis of polyurethane elastomers is outlined in Scheme 1. 2,4-Tolylene diisocyanate (2,4-TDI) and the polymerization solvent *N*,*N*-dimethylformamide (DMF, 99.8%, anhydrous) were received from Aldrich Chemical Co. and used without further purification. Poly(tetramethylene oxides) (PTMO; M_n = 650, 1000, and 2000; Aldrich) were dried in a vacuum for 2 days at 70 °C before using. The bis(azo)−diol monomer, (((((2-hydroxyethyl)ethyl)amino)phenyl)diazenyl)-phenyl sulfone, was synthesized by diazotization reaction and followed by coupling with aniline.[14]

UV−vis spectra were recorded on a Hewlett-Packard UV−vis spectrometer in DMF at room temperature. Gel permeation chromatography (GPC) analysis was performed on a Water Associates liquid chromatograph equipped with a model R401 differential refractometer using polystyrene as standards. THF was used as the eluent. Differential scanning calorimetry (DSC) measurements were done on a Perkin-Elmer DSC-6 under nitrogen atmosphere using a heating rate of 10 °C/min. The results were summarized in Table 1.

Thin films of the polyurethane elastomers were obtained by dissolving the elastomers in THF at different concentration. The solutions were filtered with 0.45 μm syringe filters and then spin-coated onto clear glass substrates with the rate of 1000 rpm. The films were allowed to dry in a vacuum oven at room temperature for 24 h. These were referred to as fresh films. Some films were annealed in a vacuum oven at 170 °C for another 24 h, which are the annealed films. After annealing, the films were allowed to cool to room temperature very

* Corresponding author. E-mail: rochon-p@rmc.ca.
† Queen's University.
‡ Current address: Xerox Research Centre of Canada, Mississauga, Ontario, Canada L5K 2L1.
§ Deceased.
|| Royal Military College.

10.1021/ma0493980 CCC: $27.50
Published on Web 06/25/2004

Scheme 1

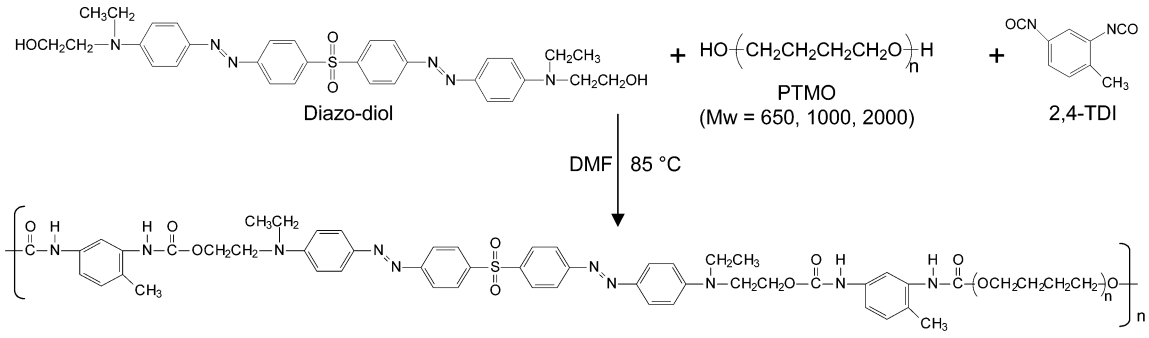

Table 1. Synthesis and Properties of the Polymers

polymer	azo in diols (wt %)	M_n of PTMO	yield (%)	azo content (wt %)[a]	M_n	M_w/M_n	film thickness (nm)
PU2	100		77	-- (78)	22 000	2.1	110 ± 5
PU2b75	75	1000	88	56 (60)	26 000	2.4	260 ± 5
PU2a50	50	650	92	39 (39)	33 000	2.4	420 ± 10
PU2b50	50	1000	87	40 (41)	34 000	2.3	430 ± 10
PU2c50	50	2000	89	42 (42)	34 000	2.4	400 ± 10
PU2b25	25	1000	82	19 (21)	26 000	2.2	680 ± 20
PU2b15	15	1000	85	11 (13)	41 000	2.2	810 ± 20

[a] The number in brace was calculated from the feed ratio.

slowly. The thickness of the films was measured by ellipsometry. The surface of the polymer films has been checked with a Nanoscope II atomic force microscopy (AFM) with contact mode. Nanoindentations were performed on elastomer annealed films with a Nanoscope E AFM using a diamond tip to determine the soft and hard domains.

The procedure for measuring the optically induced birefringence has been previously described.[8] Homogeneous films were used for the birefringence measurement and the thickness was varied from 100 to 800 nm to maintain similar absorbance. An argon laser (488 nm) with an irradiance of 65 mW/cm^2 was used as a writing light source. The birefringence was detected using a diode laser beam at 674 nm as a probe.

Surface profile gratings with a spacing of 1 μm were inscribed using contracircularly polarized interfering beams with the intensity of 250 mW/cm^2. Details about the optical setup can be found elsewhere.[9] A diode laser at 674 nm was again used as probe, and the dynamic diffraction efficiency of the first diffracted order was measured with a time resolution of 1 point/s.

Results and Discussion

Synthesis and Characterization. The polyurethane elastomers were prepared by a one-step method between diisocyanate and diols (Scheme 1). The diol monomers are an aromatic bis(azo)−diol and PTMO with the number-average molecular weight of 650, 1000, and 2000. The reaction was carried out in DMF solution at 85 °C for 48 h. Polymers were isolated by precipitation into excess methanol and purified by reprecipitation from DMF solution into methanol. Changing the molecular weight and the feed ratio of PTMO, as listed in Table 1, allowed a series of elastomers to be synthesized. To be consistent with our previous publication,[14] the model polymer without PTMO soft segments is named as **PU2**. For the elastomers, the last figure in the abbreviation represents the weight percent in the feed of the aromatic bis(azo)−diol in total diols, and **a**−**c** indicate PTMO with molecular weights of 650, 1000, and 2000, respectively. In each case, yield was higher than 75%. Molecular weight of the polyurethane elastomers varied from 26 000 to 41 000, which is comparable to those of conventional polyurethane elastomers. The polydispersity is less than 2.5 as expected for conventional condensation polymerization. Figure 1 shows UV−visible spectra of the pure **PU2** and one example of the elastomers **PU2b50** in DMF solution.

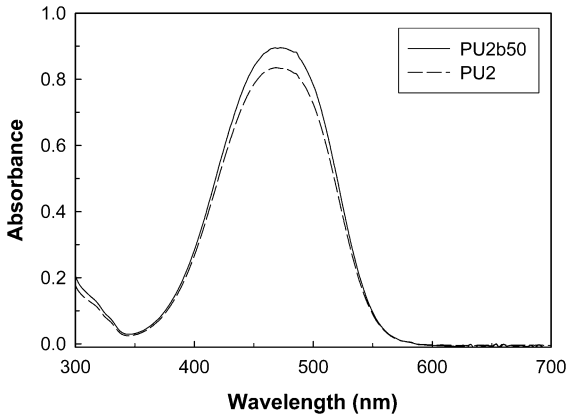

Figure 1. UV−visible spectra of the pure **PU2** and the elastomer **PU2b50** in DMF solution.

A symmetric absorption band at 488 nm is assigned to the $\pi\angle\pi^*$ transition of the azobenzene chromophore. Incorporation of the PTMO soft segment has no effect on the absorption maximum. The azo content was calculated from the absorbance on the basis of the molar extinction coefficient. The results agreed well with the values obtained from the feed ratio, which reveals that the bis(azo)−diol and PTMO have almost the same reactivity.

Thermal characterization was carried out by DSC measurement. Figure 2A shows the second heating curves of the pure **PU2** and the elastomers with different azo contents. The rigid pure **PU2** has a T_g at 167 °C. The elastomer samples were annealed at 170 °C for 24 h before measurement. When the feed of bis(azo)−diol is 50 wt %, two T_gs could be detected. The value of T_{g1} is close to that of pure PTMO 1000, while the value of T_{g2} is far lower than that of the model polyurethane **PU2**. In the other cases, only one broad T_g was observed in each curve. There are no clear endothermic changes at higher temperatures attributed to the T_g of the hard segment. This is due to the relatively small signal of the glass transition for the

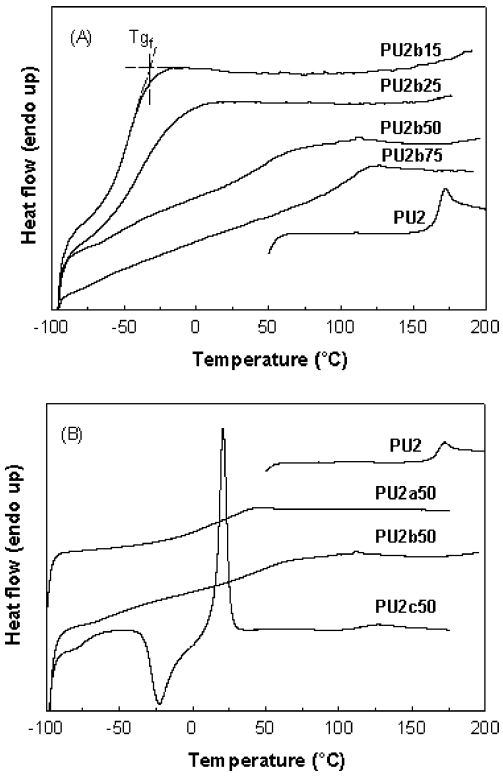

Figure 2. DSC curves (second heating) of (A) the pure **PU2** and the elastomers with different azo contents and (B) the pure **PU2** and the elastomers with different lengths of the soft segment.

hard-segment polyurethane in addition to the incomplete microphase separation in these hard-segment domains.[15,16] Nevertheless the final glass transition temperature (T_{gf}), as defined in the figure, increases with the increase of azo content. Figure 2B shows the second heating curves of the pure **PU2** and the elastomers with different PTMO as soft segment. For **PU2a50** with PTMO 650 as soft segment, only one broad T_g was observed. With the increase of molecular weight of the soft segment, a more complete microphase separation takes place. Good phase separation could be obtained when PTMO 2000 was used as soft segment. One can clearly see two T_gs in the curve. The value of T_{g1} is the same as that of pure PTMO 2000, while the T_{g2} is still lower than that of pure **PU2**, probably due to low molecular weight of the hard segment. The two peaks are assigned to crystallization and melting of the soft segment.

The surface structure of the elastomer films was characterized by AFM. Figure 3 shows the surface structure of the polymer films before and after annealing.

Before annealing, the surface is relatively homogeneous. However, one can see some particles in the fresh films, probably due to aggregation of the hard segment in THF solution. Pure **PU2** is only partially soluble in THF. Tang and co-workers also reported that polyurethane elastomers showed higher molecular weight when THF was used as eluent instead of DMF, because of the aggregation of polyurethane elastomers in THF solution.[13] After annealing, the surface became rough, with the appearance of many particles. The particle extent varied from 100 nm to several micrometers and could be as high as 350 nm. The size and the height of the particles increased with the increase of azo contents or with the increase of the molecular weight of PTMO. The results of nanoindentation experiments performed on **PU2c50** annealed film showed that the particles were composed of hard segment while the plane area is much softer. We therefore associate the formation of particles with microphase separation. DSC revealed that complete phase separation takes place in **PU2c50** only. As to the other elastomers, although DSC results showed incomplete phase separation, many particles were also observed. AFM tapping mode phase images of polyurethane elastomers were reported before.[17−19] The hard domains were very small on the order of 10 nm.

Photoinduced Birefringence. Optically induced birefringence was investigated by exposing the polymer films to a linearly polarized laser beam at 488 nm. Figure 4 shows the growth and relaxation of the photoinduced birefringence in fresh and annealed films of **PU2b50**. Birefringence could be induced in the fresh film (curve b), but the induced birefringence was not stable when the irradiation light was turned off. Only a small residual birefringence was observed. After annealing, the stability of the induced birefringence was improved significantly (curve a), and the saturation value increased slightly as well. The improvement is due to the occurrence of phase separation. As in homogeneous systems,[11] the birefringence induced in the hard domains of heterogeneous systems can be retained for an extended time. This makes it possible to use the heterogeneous materials as three-dimensional storage media.

The effects of the azo contents and the molecular weight of soft segment on photoinduced birefringence were investigated. Each sample was irradiated for 600 s at the same intensity of irradiation light. After that the induced birefringence was allowed to relax for another 600 s. Figure 5A shows the optically induced birefringence (both photostationary and stable values) as a function of azo contents. The photostationary value is defined as the one just before turning off the irradiation light, and the stable value is the one at relaxation time of 600 s.

Generally, the photostationary and the stable birefringence increase with the increase of azo contents, especially for the values obtained in annealed films. The photostationary values increase linearly with the increase of azo contents after annealing. This kind of behavior has been previously observed in copolymers containing DR1M and styrene comonomers.[20] The optically transparent soft segment has no effect on the photostationary birefringence. However, the stable birefringence deviated from a linear increase with the increase of azo contents after annealing (indicated by arrows in Figure 5A), a case that is different from the copolymers containing DR1M and styrene.[20] This may be due to low T_g of the hard domains caused by an incomplete phase separation and by low molecular weights of the hard segments. In addition, the azobenzene chromophores at the interface area of the hard and soft domains might have very low stability. Annealing has a little effect on the pure **PU2**. Both the photostationary and stable values increased slightly for elastomer **PU2b75** after annealing. In case of **PU2b50**, the photostationary value increased slightly while the stable value increased significantly after annealing. Very low signal was observed in **PU2b25** fresh film. Annealing induced remarkable increase of the photostationary and the stable values. Little or no signal could be detected

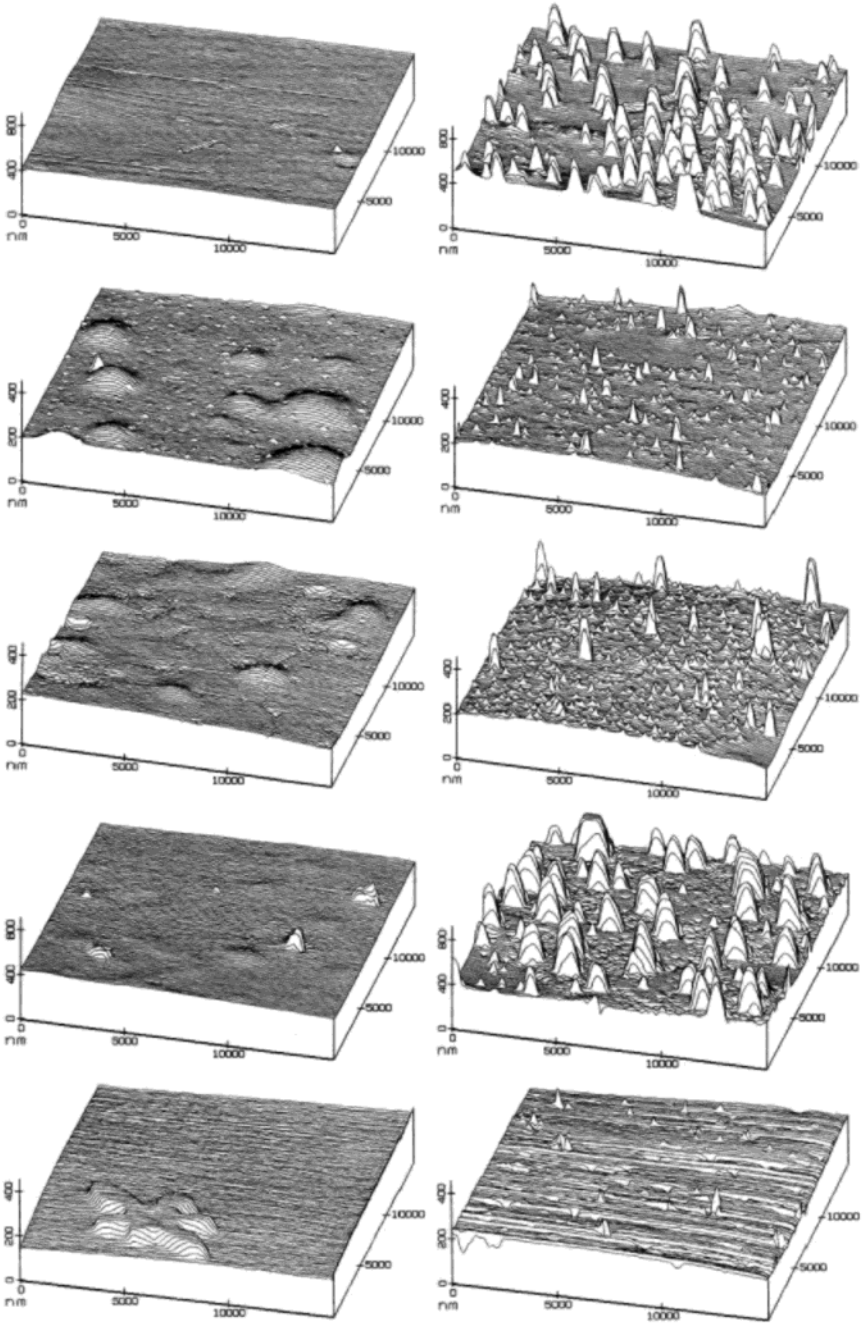

Figure 3. AFM surface profiles of the polyurethane elastomers before (left) and after (right) annealing. Samples from top to bottom: **PU2b75**; **PU2a50**; **PU2b50**; **PU2c50**; **PU2b25**.

in **PU2b15**, even in an annealed film. This is due to the incomplete phase separation and the low T_g of soft segment. In case of homogeneous systems, for instance PMMA-doped DR1,[2] birefringence was observed even at the contents of only 5 wt %.

Figure 5B shows the photostationary and stable birefringence as a function of molecular weight of PTMO. In the case of fresh films, the three elastomers show almost the same photostationary birefringence because of the similar azo contents (Table 1), but the stable value decreased with the increase of molecular weight of soft segment, since the T_g of PTMO decreases with the increase of the molecular weight. In addition, annealing produced a slight increase of the photostationary value and significant improvement of the stable values. Similar stable values for these three samples in the annealed films were expected since the three samples have the similar azo contents (Table 1). However, the absolute improvement, the difference between the stable values in the fresh and the annealed films which is calculated to be 0.005, 0.007, and 0.011 for **PU2a50**, **PU2b50**, and **PU2c50**, respectively, increased with the increase of molecular weight of PTMO

Dynamic Studies of the Photoinducing and Relaxation Processes. In a comparison of the two curves in Figure 4, it was found that the growth rate decreased while the relaxation rate increased after annealing. To investigate the kinetic behavior in detail, biexponential functions are used to analyze the growth and decay of the birefringence, as reported before.[21] The biexponential functions are

$$\Delta n = A\{1 - \exp(-k_a t)\} + B\{1 - \exp(-k_b t)\} \quad (1)$$

Table 2. Biexponential Fitting Data for the Pure PU2 and the Polyurethane Elastomers Before and After Annealing

polymer	k_a (s^{-1})	k_b (s^{-1})	A_n	B_n	k_c (s^{-1})	k_d (s^{-1})	C_n	D_n	E_n
				Before Annealing					
PU2	0.286	0.011	0.82	0.18	0.076	0.004	0.11	0.14	0.75
PU2b75	0.322	0.013	0.87	0.13	0.077	0.005	0.10	0.19	0.71
PU2a50	0.421	0.023	0.83	0.17	0.076	0.005	0.28	0.35	0.37
PU2b50	0.446	0.015	0.86	0.14	0.098	0.007	0.40	0.36	0.24
PU2c50	0.458	0.007	0.88	0.12	0.158	0.008	0.55	0.32	0.13
PU2b25	curve cannot be fitted by the biexponent ial funct ions								
				After Annealing					
PU2	0.246	0.010	0.80	0.20	0.075	0.004	0.11	0.13	0.76
PU2b75	0.249	0.011	0.81	0.19	0.085	0.005	0.11	0.17	0.72
PU2a50	0.250	0.013	0.79	0.21	0.100	0.005	0.18	0.21	0.61
PU2b50	0.253	0.015	0.80	0.20	0.112	0.006	0.18	0.19	0.62
PU2c50	0.269	0.015	0.82	0.18	0.254	0.009	0.19	0.20	0.61
PU2b25	0.524	0.020	0.85	0.15	0.226	0.007	0.46	0.22	0.32

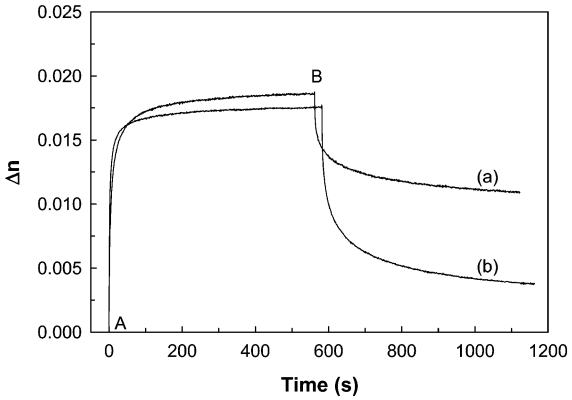

Figure 4. Typical photoinducing and relaxation curves of **PU2b50** before (b) and after (a) annealing. Linearly polarized light is turned on at point A and turned off at point B.

for photoinducing birefringence and

$$\Delta n = C \exp(-k_c t) + D \exp(-k_d t) + E \qquad (2)$$

for the relaxation process in the absence of illumination, where Δn is the birefringence observed at time t, k_a, k_b, k_c, and k_d represent the rate constants with the amplitudes of A−D, respectively. To normalize the amplitude, A_n is defined as $A/(A + B)$ and C_n is defined as $C/(C + D + E)$, etc. E_n is the fraction of birefringence conserved for a very long time. The parameters obtained by fitting the photoinducing and relaxation curves to the above two equations were summarized in Table 2.

For the writing process we find that the value of k_a increases with the increase of the contents and the molecular weight of soft segment for the fresh films. The soft segment allows the azobenzene chromophore to move more easily. The k_a of the elastomers decreased significantly after annealing due to phase separation. The formation of hard domain restricts orientation of the azobenzene chromophore. Except for **PU2b25**, the rate constants of elastomers are comparable with that of pure **PU2**. The slight increase with the increase of contents and molecular weight of the soft segment is probably due to the increase of the interface between the soft and hard segment. The reason for a large k_a observed in **PU2b25** is not clearly understood. It may be that the small dispersed hard domains in the soft matrix can undergo reorientation as a whole. Although **PU2c50** showed better phase separation, the reduction of k_a is almost the same as that of **PU2a50** and **PU2b50**.

For the relaxation process, k_c also increased with increase of the molecular weight and the contents of the soft segment for both fresh and annealed samples. Unlike the decrease of k_a, annealing induced an increase of k_c. The increased value is different for the three samples containing different PTMO. A larger increase was observed for **PU2c50**, probably due to its complete phase separation. For **PU2b25**, the behavior of fresh film could not be fitted by the biexponential functions. However, the curves of the fresh and annealed samples present a decrease of writing rate and increase of relaxation rate after annealing.

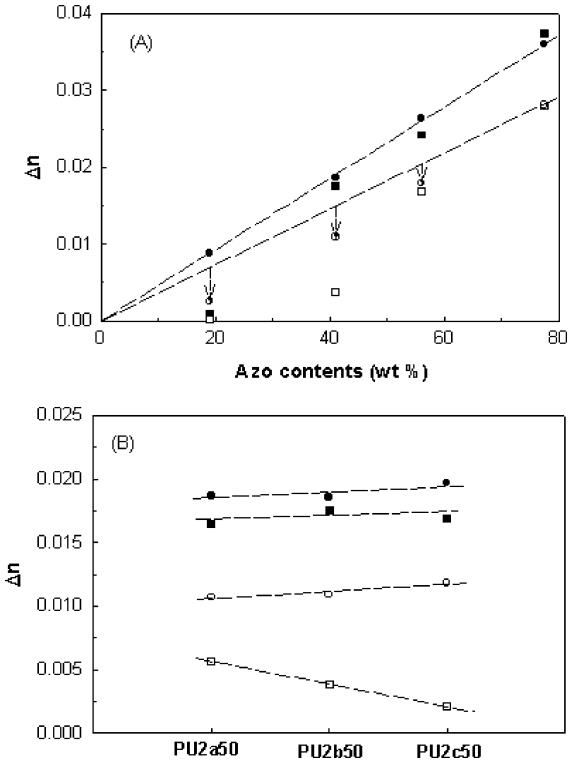

Figure 5. Photostationary (full symbols) and stable (open symbols) values of the optically induced birefringence as a function of (A) azo contents and (B) molecular weight of PTMO. Key: square, fresh sample; circle, annealed sample. The lines are only guides for eyes

Before annealing, the fast relaxation amplitude, C_n, increased, while the long-term stability, E_n, decreased with the increase of molecular weight of the soft segment, since the T_g of PTMO decreases with the increase of molecular weight. After annealing, the three polymers showed almost the same values for C_n and E_n. Annealing results in a remarkable improvement of stability of the induced birefringence, and as before, the absolute improvement increases with the increase of molecular weight of soft segment.

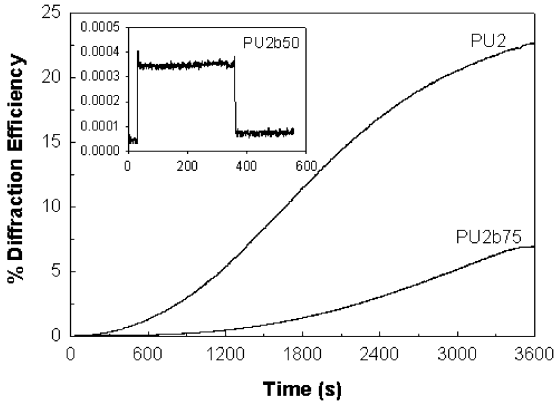

Figure 6. Diffraction efficiency of the surface relief gratings inscribed on the polymer films as a function of irradiation time. Irradiation light was turned on at 30 s and turned off at 3400 s.

Photoinduced Surface Relief Gratings. Although birefringence was induced in all polymers except for **PU2b15**, which has a very low azo content, preliminary data showed that surface relief gratings were induced only on the elastomer **PU2b75** and the model polymer **PU2**. Only a reversible volume hologram was detected in the other elastomers (Figure 6).

It may be that a continuous azo-containing phase is required for inscribing surface relief gratings. **PU2b75** has a continuous azo-containing phase (the hard phase) due to its high azo content, while the other elastomers with lower azo contents may have a dispersed azo-containing phase. Figure 6 shows the diffraction efficiency as a function of irradiation time. The thickness of the polymer films is 330 nm for **PU2** and 510 nm for **PU2b75**. Upon irradiation of the interfering beams, low efficiency diffraction (<0.4%) from volume birefringence gratings was first observed. This was followed by higher efficiency diffraction from surface relief gratings. The diffraction efficiency is about 22% for **PU2** and 7% for **PU2b75** after 1 h of irradiation. The remarkable reduction of the diffraction efficiency could not be explained solely by the lower azo contents in **PU2b75**. Since the surface relief formation requires mass movement of the polymer, segregation would seriously increase the viscosity of film thus inhibiting mass movement. In addition the presence of soft regions could help release optically induced pressure gradients thereby decreasing the force for material flow. This may be the reason no surface gratings were observed on the other elastomers.

Conclusions

A series of polyurethane elastomers containing aromatic azobenzene chromophore in the hard segment and poly(tetramethylene oxides) as soft segment was synthesized by a one-step method. DSC results showed that complete phase separation took place only in **PU2c50** with PTMO 2000 as soft segment. AMF surface study of annealed films revealed the appearance of particles composed of the hard segment These varied in size from 100 nm to several micrometers. Photoinduced birefringence and surface relief gratings were investigated in the microphase-separated systems. Birefringence could be induced in the polymers except for **PU2b15**. The stable birefringence was improved remarkably by annealing the polymer films. The stability of the birefringence increased with the increase of azo contents, while it showed almost the same value for the elastomers with different PTMO as soft segment. Dynamic studies revealed that annealing induced the decrease of k_a and increase of k_c. Surface relief gratings could be optically inscribed only on pure **PU2** and the elastomer **PU2b75**; only a reversible volume hologram was detected for the others elastomers.

Acknowledgment. Funding from the NSERC of Canada and the Department of National Defense of Canada is gratefully acknowledged. The authors thank Dr. Hugh Horton of the Department of Chemistry, Queen's University, for nanoindentation testing.

Note Added after ASAP Posting

This article was released ASAP on 6/25/2004. Figure 4 was incorrect. The correct version was posted on 7/7/2004.

References and Notes

(1) Todorov, T.; Nikolova, L.; Tomova, N. *Appl. Opt.* **1984**, *23*, 4309.
(2) Labarthet, F. L.; Sourisseau, C. *New J. Chem.* **1997**, *21*, 879.
(3) Eich, M.; Wendorff, J. H.; Reck, B.; Ringsdorf, H. *Makromol. Chem., Rapid Commun.* **1987**, *8*, 59.
(4) Stumpe, J.; Muller, L.; Kreysig, D.; Hauck, G.; Koswig, H. D.; Ruhmann, R.; Rubner, J. *Makromol. Chem., Rapid Commun.* **1991**, *12*, 81.
(5) Hvilsted, S.; Andruzzi, F.; Kulinna, C.; Siesler, H. W.; Ramanujam, P. S. *Macromolecules* **1995**, *28*, 2172.
(6) Ramanujam, P. S.; Holme, N. C. R.; Hvilsted, S. *Appl. Phys. Lett.* **1996**, *68*, 1329.
(7) Wu, Y.; Dematch, Y. Tsutsumi, O.; Shiono, T.; Ikeda, T. *Macromolecules* **1998**, *31*, 349.
(8) Natansohn, A.; Rochon, P.; Gosselin, J.; Xie, S. *Macromolecules* **1992**, *25*, 2268.
(9) Rochon, P.; Batalla, E.; Natansohn, A. *Appl. Phys. Lett.* **1995**, *66*, 136.
(10) Kim, D. Y.; Tripathy, S. K.; Li, L.; Kumar, J. *Appl. Phys. Lett.* **1995**, *66*, 1166.
(11) Natansohn, A.; Rochon, P. *Adv. Mater.* **1999**, *11*, 1387.
(12) Walkor, B. M.; Rader, C. P. *Handbook of Thermoplastic Elastomers*; Van Nostrand Reinhold: New York, 1988.
(13) Tang, W.; Farrix, R. J.; MacKnight, W. J.; Eisenbach, C. D. *Macromolecules* **1994**, *27*, 2814.
(14) Wu, Y.; Natansohn, A.; Rochon, P. *Macromolecules* **2001**, *34*, 7822.
(15) Yoshino, M.; Ito, K.; Kita, H.; Okamoto, K. *J. Polym. Sci., Part B: Polym. Phys.* **2000**, *38*, 1707.
(16) Sakurai, S.; Okamoto, Y.; Sakaue, H.; Nakamura, T.; Banda, L.; Nomura, S. *J. Polym. Sci., Part B: Polym. Phys.* **2000**, *38*, 1716.
(17) Garrett, J. T.; Runt, J.; Lin, J. S. *Macromolecules* **2000**, *33*, 6353.
(18) Kaushiva, B. D.; Wilkes, G. L. *Polymer* **2000**, *41*, 6981.
(19) Kaushiva, B. D.; Wilkes, G. L. *Polymer* **2000**, *41*, 6987.
(20) Iftime, G.; Fisher, L.; Natansohn, A.; Rochon, P. *Can. J. Chem.* **2000**, *78*, 409.
(21) Ho, M. S.; Natansohn, A.; Rochon, P. *Macromolecules* **1995**, *28*, 6124.
(22) Barrett, C. J.; Natansohn, A.; Rochon, P. *J. Phys. Chem.* **1996**, *100*, 8836.

MA0493980